PAPER

An explicitly magnetic modified embedded atom method formalism for coupled spin dynamics and molecular dynamics

To cite this article: D Dickel and M I Baskes 2025 *Modelling Simul. Mater. Sci. Eng.* **33** 015006

IOP Publishing Modelling and Simulation in Materials Science and Engineering

Modelling Simul. Mater. Sci. Eng. **33** (2025) 015006 (19pp) https://doi.org/10.1088/1361-651X/ad90f9

An explicitly magnetic modified embedded atom method formalism for coupled spin dynamics and molecular dynamics

D Dickel[1,*] **and M I Baskes**[2,3]

[1] Department of Mechanical Engineering, Mississippi State University, Starkville, MS 39759, United States of America
[2] University of North Texas, Denton, TX 76203, United States of America
[3] Los Alamos National Laboratory, Los Alamos, NM 87545, United States of America

E-mail: doyl@me.msstate.edu

Received 3 June 2024; revised 6 November 2024
Accepted for publication 11 November 2024
Published 29 November 2024

Abstract

In this paper, we augment the modified embedded atom method formalism to include magnetic spin–spin interactions for elements with a persistent magnetic moment. While previous spin coupling methods have been based on pair potentials, our Magnetic MEAM formalism, which we term MagMEAM, incorporates the many-body and angular effects of MEAM allowing for the strength of the magnetic interaction to vary with atomic environment. In particular, this allows potentials using this formalism to differentiate the magnetic interaction of different stable phases of magnetic elements such as the ferritic and austenitic phases of iron. This, in turn, allows for a more robust and realistic description of magnetism in polymorphic materials than was previously possible. The motivation for MagMEAM, including the insufficiency of magnetic pair potentials, is presented and the structure of the formalism is developed. A sample iron potential is developed using this formalism and shown to exceed the capabilities of existing magnetic pair potentials by simultaneously reproducing the magnetic energy of both martensite and austenite as well as the dynamic mechanical and magnetic properties of martensite. This newly designed formalism will allow for deeper explorations in the the complex interaction between different phases of polymorphic magnetic materials at the molecular dynamics scale.

Supplementary material for this article is available online

Keywords: modified embedded-atom method, Fe, magnetism

* Author to whom any correspondence should be addressed.

1. Introduction

Accurate predictions of the relative stability and transition pathways among different crystal phases are critically important to computational materials science. While electronic structure calculations are, in principle, capable of modeling multiple phases and the transformations among them, the computational cost associated with all but the smallest length and time scales makes them infeasible for use in dynamic simulation. A number of semi-empirical potentials, capable of relatively large length and time scales, have been able to reproduce the behavior of multiple solid phases in polymorphic materials [1–4].

Ferromagnetism, however, greatly complicates the ability of empirical interatomic potentials to model multiple phases. Even for a material as ubiquitous and essential as iron, interatomic potentials have struggled to simultaneously reproduce both the low temperature ferritic phase and the high temperature austenitic phase. This is due to the role of magnetism in stabilizing the low temperature phase [5]. Without accounting, explicitly, for the energetic contributions due to spin–spin interactions, accurate modeling of such transformations is difficult if not impossible.

Several authors have made attempts to implicitly include magnetism in the modeling of ferromagnetic elements [6–8]. While they are able to capture magnetic features associated with pure ferromagnetism at 0 K, they are unable to account for the fluctuation of magnetic moments at finite temperature as the moments are effectively fixed. More robust methods have been developed treating the magnetic moments explicitly and allowing them to evolve dynamically with time through coupled spin and molecular dynamics (SD-MD). The ability to accurately simulate spin dynamics, the evolution of the direction of magnetic moments of individual atoms, and molecular dynamics, the evolution of atomic positions, in a coupled, consistent manner was greatly enhanced by the work of Tranchida *et al* [9] with the implementation of an SD-MD formalism in LAMMPS. While the formalism can be applied to arbitrary Hamiltonians of the position and spin degrees of freedom, the magnetic contribution to the Hamiltonian has typically had the form of a pair potential, similar to the Heisenberg model [10], where the magnetic energy is a sum over pair-wise contributions of spin–spin interactions with some radial dependence. Such methods have been very effective at describing the behavior of individual phases such as ferrite [11]. Recently, a number of machine learned potentials have also been introduced which attempt to explicitly include the effects of magnetic moments. [12] introduced an extension to the moment tensor potential (MTP) formalism which included the magnitude, but not the direction, of local spins and demonstrated the improvement over nonmagnetic MTP for bcc iron. [13] used a neural network added to empirical magnetic and nonmagnetic terms to explore the behavior of defects in both bcc and FCC iron. [14] used a high dimensional neural network with features sensitive to the magnetic moment to consider collinear magnetic states in MnO. and more recently, atomic cluster expansion has been used, considering noncollinear magnetic spin vectors to reproduce many of the magnetic properties of both bcc and FCC iron [15].

Application to multiphase materials, however, has not yet been demonstrated for the SD-MD potentials. This is largely due to limitations of pair potentials to simultaneously describe the magnetic energy of multiple phases, as these energies can vary significantly, despite similar interatomic distances. An analogous barrier can be seen in the history of interatomic potential development. Until the early 1980's, empirical interatomic potentials were typically pairwise functions, and while such functions can accurately describe a number of properties within

a phase, they were poorly suited for the description of geometries with different coordinations. This was one of the factors that gave rise to the embedded atom method (EAM) [16, 17] and later the modified embedded atom method (MEAM) [18–21], which crucially included an embedding function as part of the energy contribution which was a function of the local atomic environment. This effectively made the potentials many-body and allowed for the simultaneous description of a number of material properties, including accurate energetics for multiple phases, which had not been previously possible.

Here, we follow a similar trajectory, motivated by the success of EAM and MEAM, creating a many-body magnetic potential. To do so, we extend the existing MEAM formalism to include partial electron densities which are sensitive to the relative magnetic moments of each atom. This allows, among other advantages, the simultaneous description of magnetism in multiple phases using the same interatomic potential. This formalism, which we term MagMEAM, will allow, for the first time at the classical molecular dynamics scale, dynamic calculation of polymorphic magnetic materials including the simultaneous evolution of position and spin. This will allow SD-MD calculations of realistic phase transformations in common magnetic materials that demonstrate them as well as more exotic magnetic materials. It is also possible to extend this formalism to binary or multiple element systems, as has been done successfully for MEAM [22–26], which allows for the possibility of accurately simulating, among other materials, dual phase steel alloys.

The paper is organized as follows. Section 2 outlines the limitations of magnetic pair potentials as they currently exist in the literature, using iron as a prototypical example. Section 3 presents the mathematical formulation of MagMEAM and demonstrates how it can overcome the limitations posed by pair potentials. Section 4 introduces a sample MagMEAM potential for iron and demonstrates its effectiveness in reproducing dynamic properties as well as the difference in magnetic energy between crystal structures. Section 5 summarizes and concludes the paper.

2. Magnetic pair potentials

Attempts to address magnetism at the classical molecular dynamics scale fall into two categories—implicit and explicit modeling of the magnetic moments. In the case of implicit models, the effects of magnetism are used to modify the structure of the interatomic potential, while the magnetic moment itself is not included as a dynamic variable. This was done, for example, by Ackland [6], Dudarev and Derlet [7], and Mrovec *et al* [8]. While these efforts result in a more accurate description of the ferromagnetic (FM) state, they cannot consider any other magnetic structures or magnetic fluctuations due to finite temperature, as the magnetic moment is effectively fixed. As such, these potentials will not be able to demonstrate, among other phenomena, demagnetization with increasing temperature or magnetic contributions to the specific heat. They are purely molecular dynamic methods which makes them computationally efficient, but unable to account for dynamic magnetic properties, including phase stability.

Another class of implicit magnetic models are those that consider a FM state in their data base. By fitting to this data base magnetic interactions are implicitly included in the model. As with the implicit models just discussed, these models are ineffective in prediction of 'real' magnetic effects. These models are good at predicting behavior of the FM state, but cannot address differences between different magnetic states, e.g. anti-FM (AFM) or paramagnetic. An important goal in this work is to use one of these implicit models as a base and to modify it using concepts from explicit magnetic modeling that we now discuss.

In the case of explicit modeling of magnetism, the magnetic spin is included as a dynamic variable which evolves coupled to the lattice degrees of freedom. Tranchida *et al* provide the prototypical Hamiltonian, $\mathcal{H}$, for such a system of N atoms labeled by index i:

$$\mathcal{H}(\mathbf{r},\mathbf{p},\mathbf{s}) = \mathcal{H}_{\text{mag}}(\mathbf{r},\mathbf{s}) + \sum_{i=1}^{N} \frac{p_i^2}{2m_i} + \sum_{i,j}^{N} V(\mathbf{r}) \tag{1}$$

where r_i, p_i, m_i, and s_i are the position, momentum, mass, and magnetic spin of atom i, V is a nonmagnetic, mechanical potential, and $\mathcal{H}_{\text{mag}}$ is the magnetic Hamiltonian. Typically, the magnitude of the spin is fixed with only the direction varying, introducing two additional degrees of freedom for every atom. Under the assumption of constant energy, this spin vector evolves according to

$$\frac{\mathrm{d}s_i}{\mathrm{d}t} = \omega_i \times s_i \tag{2}$$

$$\omega_i = -\frac{1}{\hbar}\frac{\partial \mathcal{H}_{\text{mag}}}{\partial s_i} \tag{3}$$

with $\hbar$ the reduced Planck constant (see [9] for more details). Previously, the form of $\mathcal{H}_{\text{mag}}$ has, following the Heisenberg model, been a pairwise summation of contributions proportional to the dot product of the individual spins:

$$\mathcal{H}_{\text{mag}} = -\mu_{\text{B}}\mu_0 \sum_{i=0}^{N} g_i s_i \cdot H_{\text{ext}} - \sum_{i\neq j}^{N} J(r_{ij})\, s_i \cdot s_j. \tag{4}$$

Here, μ_{B} and μ_0 are Bohr's magneton and the vacuum permeability respectively, g_i is the Landé factor of spin i, H_{ext} the external magnetic field and $J(r_{ij})$ a magnetic pair potential.

Additional terms proportional to powers of the dot product ($(s_i \cdot s_j)^2$ for example) have also been included to more accurately describe noncollinear spin states [27, 28]. Such explicitly magnetic formalisms have proven to be excellent tools to describe the properties of single phase materials. Nikolov *et al* [11], as an example, use a machine learned potential for FM iron plus a magnetic potential of the form given above and are able to accurately predict a number of properties for the martensitic phase.

These pairwise formalisms for $\mathcal{H}_{\text{mag}}$, however, are unsuitable for describing multiple phases [29]. We use iron as a prototypical example. As a pure element, iron is a ferromagnet with a BCC structure at room temperature and pressure. As it is heated, the magnetization decreases until its Curie temperature of 1043 K where it becomes macroscopically paramagnetic[4] At 1185 K, it undergoes a transition to γ-Fe, an FCC structure, which is also paramagnetic. As both the BCC and FCC phases are crucially important in the manufacture and design of steels and as their stability is directly dependent on magnetic contributions to the energy, it makes an ideal prototype.

We will first consider the difference in energy, as a function of volume, between FM and AFM BCC iron as determined by density functional theory (DFT) calculation. All DFT calculations are performed using VASP [31, 32] under the generalized gradient approximation as parameterized by Perdew *et al* [33] using the projector augmented-wave method for the

[4] The individual atoms still maintain their magnetic moments [30]. However, due to a loss of long-range order, the average magnetic moment in the absence of a magnetic field goes to zero.

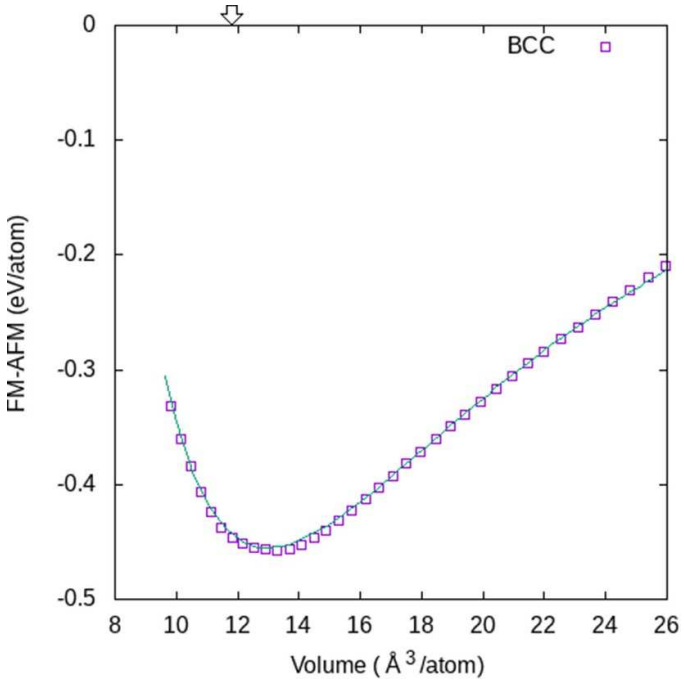

Figure 1. The energy difference between the FM and AFM magnetic orientations of BCC iron as predicted by DFT (points) and fit to the UBER equation (line). The predicted equilibrium volume for FM iron at 0 K is indicated with an arrow.

pseudopotential. For the FM case, all magnetic moments are aligned in the same direction, while for the AFM case, nearest neighbors are anti-parallel. The difference in energy as a function of volume is shown in figure 1. We can see the FM state is most energetically favorable at a lattice constant of approximately 2.96 Å with the difference decaying asymptotically for larger volumes. For small volumes, the FM state becomes relatively less favorable as predicted by Friák, Šob, and Vitek [34][5].

If we are limited to using a pair potential to describe the magnetic interaction energy, fitting to this energy difference completely specifies the form of that magnetic interaction; no additional degrees of freedom remain. Changing the number of interactions through the use of radial or angular screening cannot significantly change the result as second and third nearest neighbors in this example all have the same spin and will not contribute to the difference between FM and AFM energy, and 4th nearest neighbors, the closest which will contribute, are over 90% further away than nearest neighbors, significantly reducing their contribution.

Let us now consider the difference between FM and AFM in an FCC crystal structure. For the FCC structure, it is impossible to select an orientation where all nearest neighbors are antiparallel. Instead, for AFM, we will consider the case where spins alternate on each plane in the [001] direction, meaning 8 of the nearest neighbors will have anti-parallel spins for any given atom, as is the case for AFM BCC iron. The energy difference between FM and AFM along with the energy difference prescribed by the pair potential using the BCC energy

[5] Note that this difference closely matches the universal Binding Energy Relation (UBER) [35] curve (see curve in figure 1), which will be used in the MagMEAM formalism below.

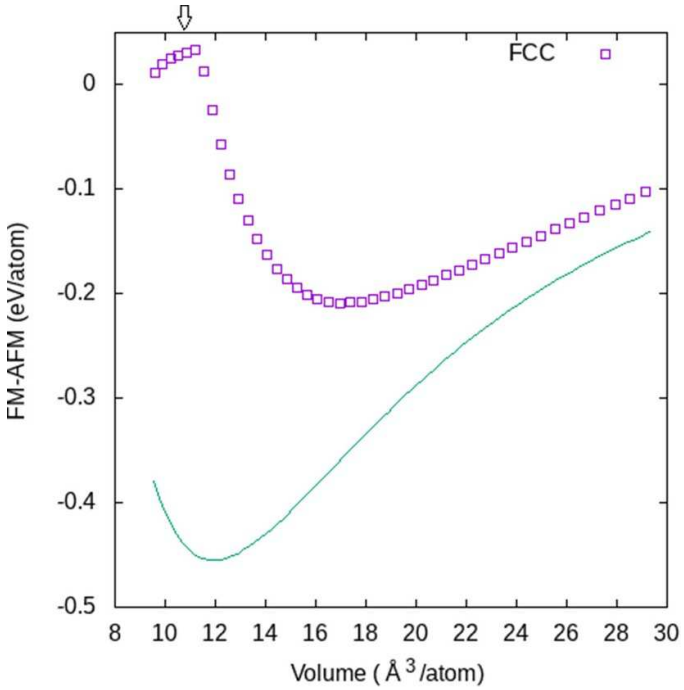

Figure 2. The energy difference between the FM and AFM magnetic orientations of FCC iron as calculated by DFT (points) and predicted by the pair potential fit to the BCC energy difference (line). The predicted equilibrium volume for FM FCC iron at 0 K is indicated with an arrow.

difference are shown in figure 2. Again, this potential is completely determined by the BCC energy difference curve given in figure 1, considering only first nearest neighbor interactions with no additional degrees of freedom. The result is that the pair potential fails to describe the magnetic interaction energy correctly. In particular, it drastically overestimates the magnetic energy at experimentally observed volumes[6].

We note the change in behavior of the energy vs. volume at small volumes. This is due to a change in the magnitude of the spin at higher pressure (smaller volume) where a smaller spin becomes the low energy state. As we will discuss below, without accounting for the change in spin magnitude, the present formalism will be unable to describe this behavior. However, the deviation will remain small compared to that given by the simple pair potential.

In order to simultaneously describe the magnetic energy of multiple phases, it is clear that a pair potential cannot be sufficient. As was done 40 years ago for nonmagnetic metals, we will now turn to the introduction of an embedding function to introduce many-body magnetic effects which will allow us to correctly reproduce the magnetic energies of multiple phases. This is done by extending MEAM to include explicitly magnetic terms both in the form of a pair potential and as partial electron densities in the embedding function.

[6] The smaller magnetic energy difference for FCC iron is not primarily due to a change in the magnitude of the magnetic moment, which is similar between FCC and BCC iron for large volumes. The FCC structure does admit a lower spin state at high compression which results in the abrupt change in behavior at small volumes.

3. The magnetic MEAM (magmeam)

The full MEAM formalism is described in appendix A along with the MagMEAM additions. Here we will focus on the modifications introduced in MagMEAM. The energy E_i of an atom i is described in MEAM by the sum of a pair potentials and an embedding function. In MagMEAM, an additional pair potential is introduced which is sensitive to the relative spins associated with each atom:

$$E_i = \frac{1}{2}\sum_{j\neq i}\phi_{ij}\left(r_{ij}\right)S_{ij} + \frac{1}{2}\sum_{j\neq i}\phi_{\mathrm{mag},ij}\left(r_{ij}\right)m_{ij}S_{m,ij} + F_i\left(\bar{\rho}_i\right). \tag{5}$$

Here, F is the embedding function, $\bar{\rho}_i$ the electron density at the site of atom i, $\phi_{ij}\left(r_{ij}\right)$ and $\phi_{\mathrm{mag},ij}\left(r_{ij}\right)$ are the nonmagnetic and magnetic pair potentials respectively, and S_{ij} and $S_{m,ij}$ are the nonmagnetic and magnetic angular screening terms. The form of the spin interaction m_{ij} is given by

$$m_{ij} = \frac{1 - s_i \cdot s_j}{2}. \tag{6}$$

In this way, the magnetic interactions all vanish from the formalism for fully FM systems, and the nonmagnetic pair potential, and indeed all of the nonmagnetic parameters, can be determined from the fully FM state where this formalism reduces exactly to MEAM. For this reason, it may be better to consider the spin interaction m_{ij} as a measure of the deviation from the FM state, instead of as a magnetic interaction. Since, in the present formalism, the magnitude of the magnetic moment of each atom, is fixed, it is not possible to consider a nonmagnetic state, and thus, magnetic interactions are always present in the formalism even if m_{ij} is zero. Note that the pair potential term is chosen to vary linearly with m. To summarize, the reference structure for the MEAM potential is taken to be FM and all MEAM parameters are obtained using this reference structure. This choice allows us to use any literature MEAM potential fit to a FM reference state as a base. The angular screening associated with the magnetic pair potential has an identical form to MEAM, but may have different parameters than the nonmagnetic one (see e.g. [19] for discussion of the angular screening interaction).

The embedding function is identical to the one used in MEAM, but the total electron density has 4 additional magnetic partial electron density terms with their own independent weight and length scale. This is similar in structure to the partial electron densities used in the multistate modified embedded atom method [36, 37] but with the additional sensitivity to magnetic moment. The form of the additional partial electron density terms is the same as MEAM. The partial electron densities are given in appendix A. The magnetic interactions are introduced to the partial electron densities through the same factor m_{ij} used in the pair potential.

As in the case of MEAM, the pair potentials are determined by fitting to reference structures. The nonmagnetic pair potential is fit to the FM structure. The magnetic pair potential is constructed to correctly reproduce the difference between the FM reference state and another non-FM state such as the AFM BCC structure described above. Assuming only first nearest neighbors are included in the calculation of the magnetic pair potential, the energy difference between the magnetic and nonmagnetic reference structures as a function of nearest neighbor distance can be written as

$$\Delta E^{\mathrm{mag}}\left(R\right) = F\left[\bar{\rho^{m0}}\left(R\right)\right] - F\left[\bar{\rho^{0}}\left(R\right)\right] + \frac{Z_1}{2}\phi_{\mathrm{mag},ij}\left(R\right) \tag{7}$$

where R is the nearest neighbor distance, Z_1 is the number of nearest neighbors with anti-parallel spins in the reference structure, and $\bar{\rho}^0(R)$ and $\rho^{\bar{m}0}(R)$ are the electron densities of the FM and non-FM reference structures respectively. The embedding energies $F[\rho]$ can be calculated directly for both FM and non-FM structure so the magnetic pair potential can be obtained as follows,

$$\phi_{\mathrm{mag},ij}(R) = \frac{2}{Z_1}\left(\Delta E^{\mathrm{mag}}(R) - F\left[\rho^{\bar{m}0}(R)\right] + F\left[\bar{\rho}^0(R)\right]\right). \tag{8}$$

As observed above, the form of ΔE^{mag} is well approximated by the universal Binding Energy Relation [35]. As such, this form is used in the MagMEAM formalism, characterized by 3 parameters: E_{mag},α_{mag}, and r_{mag}

$$\Delta E^{\mathrm{mag}}(R) = -E_{\mathrm{mag}}\left(1+\alpha_{\mathrm{mag}}\left(\frac{R}{r_{\mathrm{mag}}}-1\right)\right)e^{\left[-\alpha_{\mathrm{mag}}\left(\frac{R}{r_{\mathrm{mag}}}-1\right)\right]}. \tag{9}$$

As in the case of just a pair potential for the magnetic interaction, the difference between FM and AFM for a given structure will now be exactly reproduced through the parameterization of the magnetic UBER equation. This leaves the weights and length scales for the magnetic partial electron densities, as well as the magnetic screening parameters, as free parameters to reproduce other magnetic behavior.

Although only a unary potential is considered here, the extension to binary systems is straightforward and follows the MEAM formalism exactly. To extend a pair of magnetic unary potentials to a binary potnetial, a new magnetic pair potential is defined which correctly reproduces the magnetic energy difference for some non-FM binary reference structure, and new magnetic screening parameters among different elemental species can be introduced. Otherwise, no new parameters are required to extend two unary potentials to a binary.

We briefly note a few of the limitations of this formalism. While MagMEAM allows for the variation in magnetic energy between different phases or coordinations, it cannot account for all magnetic phenomena. Most notably, it assumes that the magnitude of the magnetic moment of each atom is fixed. While this might be approximately true even between different phases, it will fail to correctly characterize cases where the magnitude of the spin changes. As an example, FM FCC iron is known to have two different stable spin states, depending on the volume, resulting in two stable minima in a calculation of its energy vs. volume [15, 38]. MagMEAM can only reproduce one of these spin states. For this work, we choose to fit to the larger volume, high spin state. Similarly, the magnetic moment is known to be suppressed at high compression as a result of Pauli exclusion. This means that the magnetic energy difference should vanish at small volumes or in regions of high electron density. MagMEAM will instead predict, in accordance with the UBER equation used to derive the pair potential, that the AFM state becomes increasingly favorable at small volumes. This energy difference is quite small compared to the total energy at these pressures, however, so it should not significantly affect the dynamic behavior. Finally, due to the inability of MagMEAM to consider longitudinal fluctuations in the magnetic moment of each atom, it fails to capture much of the innovation of earlier physics based approaches [6–8] which, while only treating the magnetic moment implicitly, did consider the magnetic energy landscape in their formulation, and as such, lacks many of their physical insights.

Table 1. MagMEAM potential parameters for the prototype Fe potential. The units of the cohesive energies, E_c and E_{mag}, and the lattice parameters, a_{lat} and $r_{0,\mathrm{mag}}$ are eV and Å, respectively.

E_c	r_{lat}	α	$\beta^{(0)}$	$\beta^{(1)}$	$\beta^{(2)}$	$\beta^{(3)}$	$t^{(1)}$	$t^{(2)}$	$t^{(3)}$	C_{min}	C_{max}	A
4.28	2.4725	5.138	6.31	5.96	5.78	2.98	25.0	16.55	10.0	0.4831	2.525	0.9
E_{mag}	$r_{0,\mathrm{mag}}$	α_{mag}	$\beta^{m(0)}$	$\beta^{m(1)}$	$\beta^{m(2)}$	$\beta^{m(3)}$	$t^{m(0)}$	$t^{m(1)}$	$t^{m(2)}$	$t^{m(3)}$	C_{magmin}	C_{magmax}	$t^{m(00)}$
0.46	2.5543	6.796	7.0	6.5	0.5	0.0	0.45	1.0	0.2	0.0	1.9	2.9	−0.94

The authors have implemented the MagMEAM formalism in LAMMPS [39]. The potential files closely follow the format used for MEAM. The potential files for the potential presented below and a sample input script using the potential have been included in the supplemental material. The source code for the MagMEAM potential style can be found on Github (https://github.com/DoylD/MagMEAM).

4. A sample magMEAM potential for iron

As a demonstration of the use of the MagMEAM formalism to model the magnetic properties of multiple crystal phases simultaneously, we parameterize a potential for iron which correctly reproduces the magnetic energy differences described above for several phases simultaneously.

The parameters for the base MEAM potential, which uses the FM BCC structure as the reference state and the additional MagMEAM parameters are given in table 1. The base MEAM potential was constructed to show agreement with the FM BCC and high spin FM FCC structures, including the relative energy, elastic constants, and Bain transformation pathway. The AFM BCC structure is used as the reference state for the magnetic contribution, and E_{mag}, $r_{0,\mathrm{mag}}$, and α_{mag} are determined by reproducing the energy difference between FM and AFM for the BCC structure as shown previously in figure 1. As discussed above, the formalism ensures that this relationship will be maintained regardless of the choice of other magnetic parameters. We next demonstrate the properties of this potential at 0 K.

4.1. Molecular statics properties

The energy of the BCC structure for both FM and AFM magnetic configurations matches the results from DFT by construction. For FCC, the energy difference as a function of volume between the FM phase and each AFM phase is shown in figure 3. The prediction of the pure pair potential shown in figure 2 is given for comparison. While the MagMEAM prediction does not exactly match the DFT results, the agreement is considerably improved from the pair potential prediction. In particular, at experimentally relevant volumes, the AFM phase become stable relative to the FM phase. Additionally, the difference in the FM and AFM phases is close to first principles results overall, even for volumes where FM is lower energy. Since the FCC phase has a theoretical Néel temperature of less than 100 K [40, 41], the exact 0 K magnetic ordering is not of key importance at temperatures where that phase is stable. What is relevant is the drastically reduced magnetic energy as compared to the prediction of the pair potential. This decreases the energy of the paramagnetic FCC phase compared to the paramagnetic BCC phase, improving its relative stability.

Table 2. Material properties for BCC and FCC FM and antiFM configurations as predicted by the MagMEAM potential and compared with DFT or experimental results. DFT value are given in italics. ΔE is the per atom energy difference between the given phase and the ground state of FM BCC.

Property	DFT/Experiment	MagMEAM
BCC-FM		
E_c (eV)	4.28	4.28
a (Å)	2.855	2.855
B (GPa)	170.4[a]	173.1
C' (GPa)	51.9[a]	52.6
C_{44} (GPa)	120.75[a]	121.80
BCC-AFM		
ΔE (meV)	438	444
a Å	2.80	2.82
FCC-FM		
ΔE (meV)	163	141
a Å	3.63	3.59
FCC-AFM		
ΔE (meV)	113	150
a Å	3.48	3.43

[a] Adams [42]

Table 2 shows a brief summary of 0 K properties for FM and AFM magnetic orderings for several crystal and magnetic structures in comparison with first principles. Again, the improvement over a pair potential for the FCC phase is significant.

4.2. Spin dynamic-molecular dynamic behavior

In order to test the behavior of this sample potential at finite temperature, a number of SD-MD simulations were performed for a periodic $10 \times 10 \times 10$ BCC supercell following the method presented by Tranchida *et al*. However, that work used a numerical integration scheme that assumed a simple pair potential style for the magnetic interaction. It was necessary to extended this integration scheme here to account for the more complex magnetic formalism. This extension is discussed in appendix B.

The other limitation of the SD-MD formalism is that it cannot be directly coupled to a barostat [9], allowing the periodic box dimensions to change in response to pressure resulting from increasing temperature. Following [11], we alternated using both spin and molecular dynamics with only using molecular dynamics and a coupled barostat, allowing the pressure to equilibrate. The temperature of each simulation was maintained with a langevin thermostat and the relevant quantities averaged over the last 20 ps of a 100 ps simulation. The results for the elastic constants, magnetization, thermal expansion, and specific heat are shown in figures 4 and 5. Of note are the excellent agreement with experiment for thermal expansion, the demagnetization with temperature and a predicted Curie temperature of 1015 K, compared to 1044 K observed experimentally, and the change in specific heat through this second order phase transition. Additionally, the behavior of the shear elastic constant, C', is seen to decrease significantly as the material moves through the Curie temperature in both the MagMEAM potential and experiment. As this softening is directly correlated with the decrease in total magnetic moment for the MagMEAM potential, it is likely related to the relatively lower energy of the

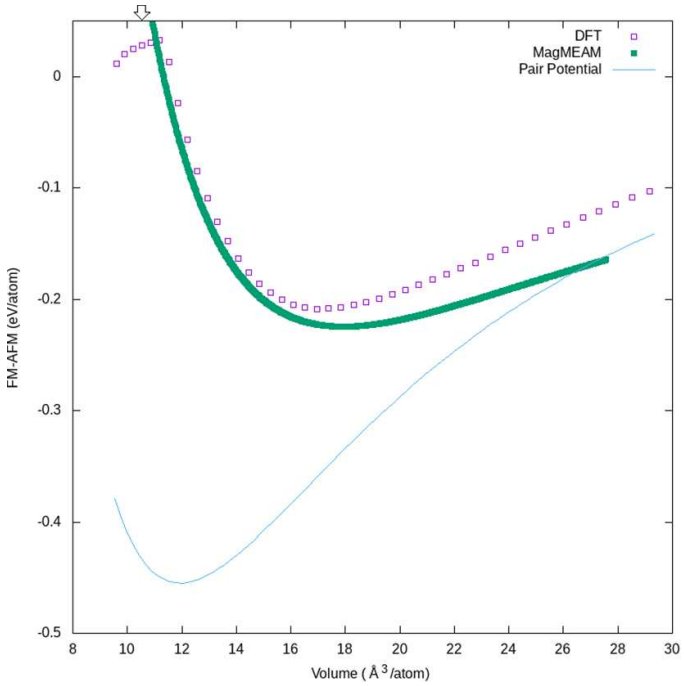

Figure 3. The energy difference between the FM and AFM magnetic orientations of FCC iron as predicted by DFT (points) and from the fit MagMEAM potential (line). The predicted equilibrium volume for FM iron at 0 K is indicated with an arrow.

FCC AFM state as compared to BCC AFM. This energetic bias will tend to decrease the restoring force along the [110] direction and may facilitate a transformation to the FCC phase. The MagMEAM potential also shows considerable softening of the C_{44} elastic constant, suggesting another additional transformation mode. At elevated temperature, no spontaneous transformation to the FCC phase was observed, however. This may be due to the inability to couple spin dynamics to a barostat, or the short time duration of the simulations, limited by the sequential nature of spin integration in the scheme employed by LAMMPS [9].

5. Conclusion

We present the MagMEAM SD-MD interatomic potential formalism. This formalism is an extension of the traditional MEAM, including a magnetic pair potential and partial electron densities which are sensitive to the spin of individual atoms. In particular, magnetic terms are introduced which are zero in the case of ferromagnetism, all spins being aligned, and nonzero otherwise. This allows the FM state to be used as a basis for the non-magnetic parameters in the potential and more complex magnetic configurations to determine those sensitive to moment.

This formalism is a significant advancement over the explicitly magnetic potentials strictly using pair potentials to describe the magnetic interaction which exist in the literature. We demonstrate that pair potentials are necessarily insufficient to simultaneously describe the magnetic energies for multiple crystal phases using iron as a test case. This makes the previously existing formalisms defective with regard to polymorphic elements where dual-phase materials or phase transitions are important to understand. This determination motivated a

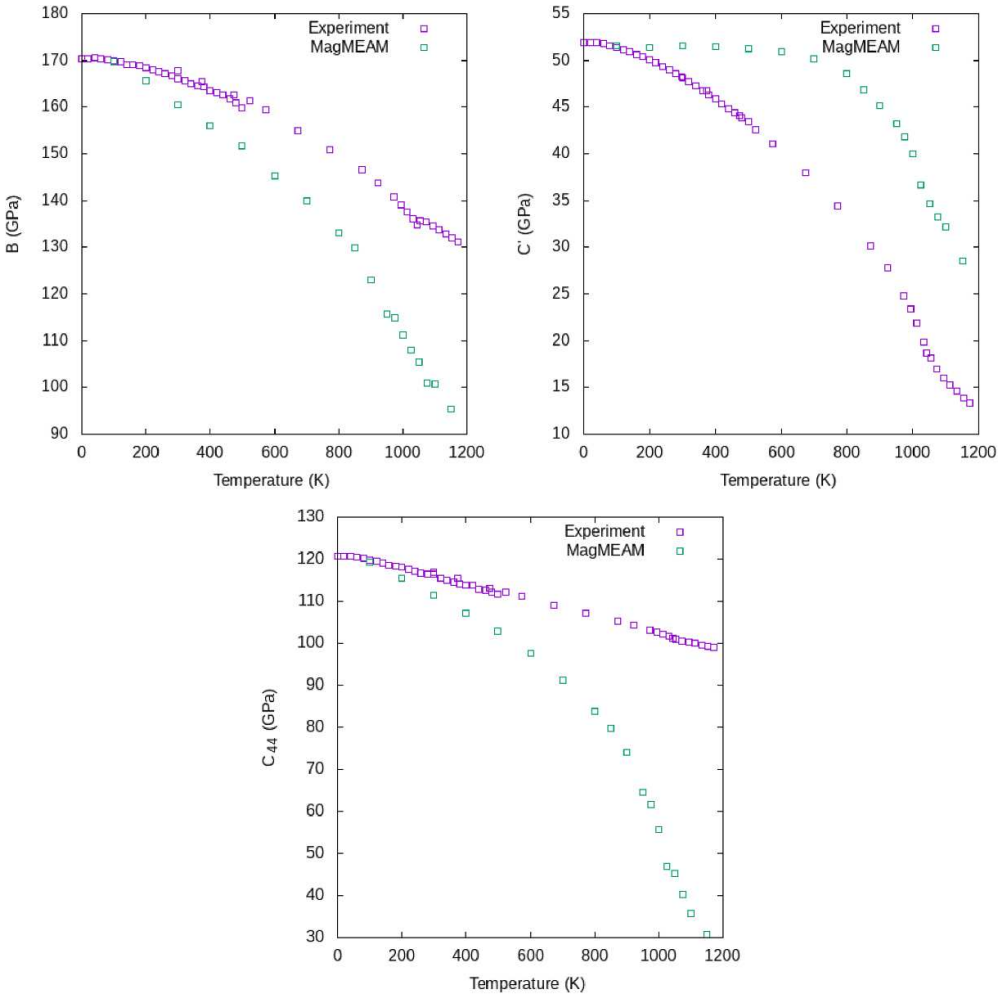

Figure 4. (a) The bulk modulus, (b) C' shear elastic constant, and (c) C_{44} elastic constant as predicted by the MagMEAM potential and observed experimentally. Experiment values are from [42, 43].

many-body formalism for magnetic interactions with MEAM being chosen as a template due to its previous successes describing polymorphic elements.

We next present an application of this formalism to Fe, which experimentally exhibits a transition between BCC and FCC that is both crucially important in metallurgy and industry and also heavily dependent on magnetism. We demonstrate that the MagMEAM potential we present for Fe reproduces the difference between FM and AFM magnetic configurations as predicted by DFT for the BCC and FCC crystal phases. Additionally, the potential can be used in dynamic calculation to reproduce many of the finite temperature behaviors of BCC iron, including the magnetization vs. temperature and Curie temperature. The MagMEAM formalism can be extended in a straightforward manner to binary systems and more complicated

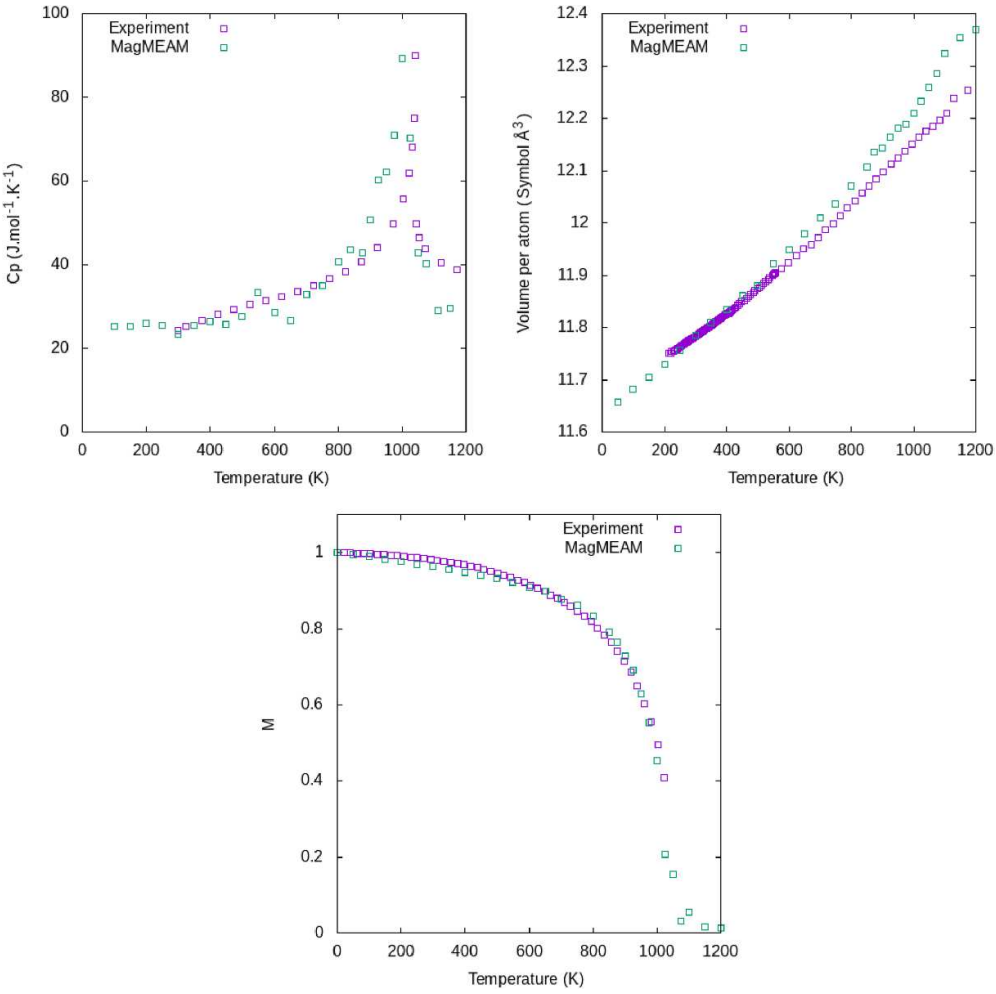

Figure 5. (a) The specific heat , (b) atomic volume, and (c) magnitude of the total magnetic moment as predicted by the MagMEAM potential and observed experimentally. Experiment values are from [44–48].

alloys included rare-earth magnets. MagMEAM should represent an important step forward in the modeling of magnetic materials at the nanoscale.

Data availability statement

The data cannot be made publicly available upon publication because no suitable repository exists for hosting data in this field of study. The data that support the findings of this study are available upon reasonable request from the authors.

Appendix A. The magnetic MEAM (MagMEAM) formalism

In the MagMEAM formalism, the potential energy of a system, $U(\{\vec{r}_i\})$, is given by

$$U(\{r_i\}) = \sum_i \left[F_i[\bar{\rho}_i] + \frac{1}{2}\sum_{j(\neq i)} S_{ij}\Phi(r_{ij}) + \frac{1}{2}\sum_{j(\neq i)} S_{m,ij}\Phi_m(r_{ij})\, m_{ij} \right] \tag{10}$$

where $F_i(\bar{\rho}_i)$ is the embedding energy to insert an atom i located at r_i into the background electron density $\bar{\rho}_i$, and $\Phi(r_{ij})$ and $\Phi_m(r_{ij})$ are pair interactions between atoms i and j, separated by the vector $\vec{r}_{ij}$ with length r_{ij}, and m_{ij} is the spin–spin interaction defined in the main text. The energy per atom of a particular FM reference structure can be written as

$$U_i^u(r) = F_i\left(\bar{\rho}_i^0(r)\right) + \frac{Z}{2}\Phi(r) \tag{11}$$

if considering only nearest neighbors, where $\bar{\rho}_i^0(r)$ is the background density at the center of atom i obtained from the superposition of the densities of the neighboring atoms, and Z is the number of nearest neighbors. For second nearest neighbors, the above equation is modified as in [20]. The energy, $U_i^u(r)$, is assumed take the form of the universal equation of state initially given by Rose [35] and modified by Baskes [49]:

$$U_i^u(r) = -E_c\left[1 + a^*(r)\right] e^{-a^*(r)} \tag{12}$$

$$a^*(r) = \alpha\left(\frac{r}{r_e} - 1\right) \tag{13}$$

$$\alpha = \left(\frac{9\Omega B}{E_c}\right)^{\frac{1}{2}} \tag{14}$$

where E_c, r_e, Ω, and B, are the cohesive energy, nearest-neighbor distance, atomic volume, and bulk modulus of the element in the reference structure. Equations (11) through (14) are used to determine Φ.

The energy for an AFM reference structure is found similarly as

$$U_i^u(r) = F_i\left(\bar{\rho}_i^0(r)\right) + \frac{Z}{2}\Phi(r) + \frac{Z_m}{2}\Phi_m(r) \tag{15}$$

where Z_m is the number of nearest neighbors with antiparallel spin. Here, the difference between the energy of the FM and AFM structure is also assumed to follow equation (12). The embedding function is defined as

$$F_i[\bar{\rho}_i] = AE_c\bar{\rho}_i \ln\bar{\rho}_i \tag{16}$$

where A is an adjustable parameter in the model. This relation is motivated in an attempt to empirically reproduce the logarithmic relation between bond length and number of bonds [50].

In MagMEAM, the electron density is given by a superposition of angularly dependent nonmagnetic and magnetic partial electron densities and depends on the relative position of any three atoms via Legendre polynomials, P_l:

$$\left(\rho_i^{(l)}\right)^2 = \sum_{j(\neq i)} \rho_j^{a(l)}\left(r_{ij}\right) \sum_{k(\neq i)} \rho_k^{a(l)}\left(r_{ik}\right) P_l\left(\cos\theta_{ijk}\right) S_{ij} S_{ik} \tag{17}$$

$$\left(\rho_i^{m(l)}\right)^2 = \sum_{j(\neq i)} \rho_j^{am(l)}\left(r_{ij}\right) \sum_{k(\neq i)} \rho_k^{am(l)}\left(r_{ik}\right) P_l\left(\cos\theta_{ijk}\right) S_{m,ij} S_{m,ik} m_{ij} \tag{18}$$

$$\cos\theta_{ijk} = \frac{\vec{r}_{ij}\cdot\vec{r}_{ik}}{|r_{ij}|\,|r_{ik}|} \tag{19}$$

where $\rho_j^{a(l)}$ are the atomic electron density contributions from atom j to atom i, θ_{ikj} is the angle between atoms i, j, and k, and l varies from 0 to 3. The electron densities are assumed to exponentially decay with increasing distance:

$$\rho_j^{a(l)}\left(r_{ij}\right) = \exp\left[-\beta^{(l)}\left(\frac{r_{ij}}{r_e} - 1\right)\right] \tag{20}$$

where $\beta^{(l)}$ are decay constant free parameters in the model. In order to better reproduce experimental and DFT results for iron, it was found useful to introduce an additional term proportional to both $\rho_i^{m(0)}$ and $\rho_i^{(0)}$. Such a term is sensitive to both the total number of neighbors as well as the number of neighbors with differing spin, making it useful in distinguishing AFM BCC and FCC phases. Combining the partial electron densities is accomplished by means of a function $G(\Gamma)$:

$$\overline{\rho}_i = \rho_i^{(0)} G\left(\Gamma_i\right) \tag{21}$$

where $G(\Gamma)$ defines the angular dependence, and Γ contains the components of the total density

$$\Gamma_i = \sum_{l=1}^{3} t^{(l)} \left(\frac{\rho_i^{(l)}}{\rho_i^{(0)}}\right)^2 + \sum_{l=0}^{3} t^{m(l)} \left(\frac{\rho_i^{m(l)}}{\rho_i^{(0)}}\right)^2 + t^{m(00)} \frac{\rho_i^{m(0)}}{\rho_i^{(0)}} \tag{22}$$

where the $t^{(l)}$, $t^{m(l)}$, $t^{m(00)}$ are nonmagnetic and magnetic weighting parameters of the model.

MEAM allows some flexibility in the form of $G(\Gamma)$ with different choices being used for different potentials [19]. For the Fe potential presented here we use

$$G\left(\Gamma\right) = \frac{2}{1+e^{-\Gamma}}. \tag{23}$$

Finally, MEAM truncates the interaction of distant atoms by means of a screening function. Screening by multiple atoms is multiplicative, such that the total screening of the interaction between atoms i and j, S_{ij}, is the product of the screening, S_{ikj}, due to all atoms k:

$$S_{ij} = \prod_{k(\neq i,j)} S_{ikj} \tag{24}$$

S_{ikj}, which is based on a simple geometric consideration, is given by

$$S_{ikj} = f_c\left(\frac{C_{ikj} - C_{\min}}{C_{\max} - C_{\min}}\right) \tag{25}$$

where $C_{\min}$ and $C_{\max}$ define the limiting values of C_{ikj}, which is determined by the equation of an ellipse of radius $r_{ij}/2$ with atom k on it:

$$C_{ikj} = \frac{2\left(X_{ik} + X_{kj}\right) - \left(X_{ik} - X_{kj}\right)^2 - 1}{1 - \left(X_{ik} - X_{kj}\right)^2} \tag{26}$$

where $X_{ik} = (r_{ik}/r_{ij})^2$ and $X_{kj} = (r_{kj}/r_{ij})^2$. $f(x)$ is the smooth function of x:

$$f_c(x) = \begin{cases} 1 & \text{for } x \geqslant 1 \\ \left[1 - (1-x)^4\right]^2 & \text{for } 0 < \mathrm{x} < 1 \\ 0 & \text{for } x \leqslant 0. \end{cases} \tag{27}$$

Thus, if $S_{ij} = 1$, the atoms are unscreened, while for $S_{ij} = 0$ they are completely screened. The magnetic screening, used for the magnetic pair potential and magnetic partial electron densities functions identically but can, in principle, use different values of $C_{\max}$ and $C_{\min}$.

Appendix B. Numerical integration

As discussed in Tranchida *et al*, dynamic evolution of the spins must be performed sequentially, with one spin being updated at a time. In order to conserve total energy up to order Δt^2 in the timestep, the change in the spin, s_i of atom i over some timestep Δt is given by a series expansion:

$$s_i(t + \delta t) = s_i(t) + \delta t \frac{\mathrm{d}s_i}{\mathrm{d}t} + \frac{1}{2}\delta t^2 \frac{\mathrm{d}^2 s_i}{\mathrm{d}t^2}. \tag{28}$$

The result is then normalized to ensure that the magnitude of the spin remains unchanged. This result can be rewritten in terms of the spin force, ω_i where:

$$\omega_i = \frac{\mathrm{d}H}{\mathrm{d}s_i} \tag{29}$$

$$\frac{\mathrm{d}s_i}{\mathrm{d}t} = \omega_i \times s_i \tag{30}$$

where H is the Hamiltonian of the system. Thus the numerical integrator becomes

$$s_i(t + \delta t) = s_i(t) + \delta t(\omega_i \times s_i) + \frac{1}{2}\delta t^2 \left(\frac{\mathrm{d}\omega_i}{\mathrm{d}t} \times s_i + \omega_i \times \frac{\mathrm{d}s_i}{\mathrm{d}t}\right). \tag{31}$$

The δt^2 term has two components. The derivative in the second can again be rewritten in terms of ω_i. For a simple magnetic pair potential such as that given in equation (4), the first component will vanish as ω_i in that case will not be a function of s_i and only s_i is allowed to evolve during the integration as the spins are updated sequentially, as mentioned above. Therefore, this terms is not included by Tranchida *et al*. However, for a more complex magnetic

Hamiltonian, it must be included to ensure energy conservation. We rewrite the derivative $\frac{d\omega_i}{dt}$ as:

$$\frac{d\omega_i}{dt} = \frac{d\omega_{i,\alpha}}{ds_{i,\beta}} \frac{ds_{i,\beta}}{dt} = \frac{d^2H}{ds_{i,\alpha} ds_{i,\beta}} \omega_{i,\gamma} s_{i,\delta} \epsilon_{\gamma\delta\beta} \tag{32}$$

where $s_{i,\alpha}$ and $\omega_{i,\alpha}$ denote the α component of the vectors s_i and ω_i respectively, Einstein summation is assumed over repeated indicies, and ε is the Levi-Civita tensor. These second derivative contributions are calculated analytically and included in the numerical integrator used for dynamic calculation.

ORCID iD

D Dickel https://orcid.org/0000-0003-1259-6887

References

[1] Hennig R G, Lenosky T J, Trinkle D R, Rudin S P and Wilkins J W 2008 Classical potential describes martensitic phase transformations between the α, β and ω titanium phases *Phys. Rev.* B **78** 054121
[2] Mendelev M I, Underwood T L and Ackland G J 2016 Development of an interatomic potential for the simulation of defects, plasticity and phase transformations in titanium *J. Chem. Phys.* **145** 154102
[3] Dickel D, Barrett C D, Carino R L, Baskes M I and Horstemeyer M F 2018 Mechanical instabilities in the modeling of phase transitions of titanium *Modelling Simul. Mater. Sci. Eng.* **26** 065002
[4] Lee T, Baskes M I, Valone S M and Doll J D 2012 Atomistic modeling of thermodynamic equilibrium and polymorphism of iron *J. Phys.: Condens. Matter* **24** 225404
[5] Herper H C, Hoffmann E and Entel P 1999 *Ab initio* full-potential study of the structural and magnetic phase stability of iron *Phys. Rev.* B **60** 3839
[6] Ackland G J 2006 Two-band second moment model for transition metals and alloys *J. Nucl. Mater.* **351** 20–27
[7] Dudarev S L and Derlet P M 2005 A 'magnetic'interatomic potential for molecular dynamics simulations *J. Phys.: Condens. Matter* **17** 7097
[8] Mrovec M, Nguyen-Manh D, Elsässer C and Gumbsch P 2011 Magnetic bond-order potential for iron *Phys. Rev. Lett.* **106** 246402
[9] Tranchida J, Plimpton S J, Thibaudeau P and Thompson A P 2018 Massively parallel symplectic algorithm for coupled magnetic spin dynamics and molecular dynamics *J. Comput. Phys.* **372** 406–25
[10] Heisenberg W 1985 Zur Theorie des Ferromagnetismus *Original Scientific Papers Wissenschaftliche Originalarbeiten* (Springer) pp 580–97
[11] Nikolov S, Wood M A, Cangi A, Maillet J-B, Marinica M-C, Thompson A P, Desjarlais M P and Tranchida J 2021 Data-driven magneto-elastic predictions with scalable classical spin-lattice dynamics *npj Comput. Mater.* **7** 1–12
[12] Novikov I, Grabowski B, Körmann F and Shapeev A 2022 Magnetic moment tensor potentials for collinear spin-polarized materials reproduce different magnetic states of bcc fe *npj Comput. Mater.* **8** 13
[13] Chapman J B J and Ma P-W 2022 A machine-learned spin-lattice potential for dynamic simulations of defective magnetic iron *Sci. Rep.* **12** 22451
[14] Eckhoff M and Behler J 2021 High-dimensional neural network potentials for magnetic systems using spin-dependent atom-centered symmetry functions *npj Comput. Mater.* **7** 170
[15] Rinaldi M, Mrovec M, Bochkarev A, Lysogorskiy Y and Drautz R 2024 Non-collinear magnetic atomic cluster expansion for iron *npj Comput. Mater.* **10** 12
[16] Daw M S and Baskes M I 1984 Embedded-atom method: Derivation and application to impurities, surfaces and other defects in metals *Phys. Rev.* B **29** 6443

[17] Daw M S, Foiles S M and Baskes M I 1993 The embedded-atom method: a review of theory and applications *Mater. Sci. Rep.* **9** 251–310
[18] Baskes M I 1992 Modified embedded-atom potentials for cubic materials and impurities *Phys. Rev.* B **46** 2727
[19] Baskes M I 1997 Determination of modified embedded atom method parameters for nickel *Mater. Chem. Phys.* **50** 152
[20] Lee B-J and Baskes M I 2000 Second nearest-neighbor modified embedded atom method potential *Phys. Rev.* B **62** 8564
[21] Lee B-J, Baskes M I, Kim H and Cho Y K 2001 Second nearest-neighbor modified embedded atom method potentials for BCC transition metals *Phys. Rev.* B **64** 184102
[22] Kim Y-M and Lee B-J 2008 Modified embedded-atom method interatomic potentials for the Ti-C and Ti–N binary systems *Acta Mater.* **56** 3481
[23] Sa I and Lee B-J 2008 Modified embedded-atom method interatomic potentials for the Fe-Nb and Fe-Ti systems *Scr. Mater.* **59** 595–8
[24] Kim H-K, Jung W-S and Lee B-J 2009 Modified embedded-atom method interatomic potentials for the Fe–Ti–C and Fe–Ti–N ternary systems *Acta Mater.* **57** 3140–7
[25] Kim K-H, Bae Jeon J B and Lee B-J 2015 Modified embedded-atom method interatomic potentials for MG–X (X = Y, SN, CA) binary systems *Calphad* **48** 27–34
[26] Kim Y-K, Kim H-K, Jung W-S and Lee B-J 2016 Atomistic modeling of the Ti–Al binary system *Comput. Mater. Sci.* **119** 1–8
[27] Rosengaard N M and Johansson B 1997 Finite-temperature study of itinerant ferromagnetism in Fe, Co and Ni *Phys. Rev.* B **55** 14975
[28] Szilva A, Costa M, Bergman A, Szunyogh L, Nordström L and Eriksson O 2013 Interatomic exchange interactions for finite-temperature magnetism and nonequilibrium spin dynamics *Phys. Rev. Lett.* **111** 127204
[29] Chapman J B J, Ma P-W and Dudarev S L 2020 Effect of non-heisenberg magnetic interactions on defects in ferromagnetic iron *Phys. Rev.* B **102** 224106
[30] Zhang H, Johansson B and Vitos L 2011 Density-functional study of paramagnetic iron *Phys. Rev.* B **84** 140411
[31] Kresse G and Joubert D 1994 From ultrasoft pseudopotentials to the projector augmented-wave method *Phys. Rev.* B **59** 1758
[32] Kresse G and Furthmüller J 1996 Efficient iterative schemes for ab initio total-energy calculations using a plane-wave basis set *Phys. Rev.* B **54** 11169
[33] Perdew J P, Chevary J A, Vosko S H, Jackson K A, Pederson M R, Singh D J and Fiolhais C 1992 Atoms, molecules, solids and surfaces: applications of the generalized gradient approximation for exchange and correlation *Phys. Rev.* B **46** 6671
[34] Friák M, Šob M and Vitek V 2001 *Ab initio* calculation of phase boundaries in iron along the bcc-FCC transformation path and magnetism of iron overlayers *Phys. Rev.* B **63** 052405
[35] Rose J H, Smith J R, Guinea F and Ferrante J 1984 Universal features of the equation of state of metals *Phys. Rev.* B **29** 2963
[36] Baskes M I, Srinivasan S G, Valone S M and Hoagland R G 2007 Multistate modified embedded atom method *Phys. Rev.* B **75** 094113
[37] Valone S M, Baskes M I and Rudin S P 2012 Stacking fault energy in FCC plutonium with multiple reference states in the modified embedded atom method *J. Nucl. Mater.* **422** 20–26
[38] Mryasov O N, Liechtenstein A I, Sandratskii L M and Gubanov V A 1991 Magnetic structure of FCC iron *J. Phys.: Condens. Matter* **3** 7683
[39] Plimpton S J 1995 Fast parallel algorithms for short-range molecular dynamics *J. Comput. Phys.* **117** 1–19
[40] Huang W 1989 An assessment of the Fe-Mn system *Calphad* **13** 243–52
[41] La Roca P, Marinelli P, Baruj A, Sade M and Fernández Guillermet A 2016 Composition dependence of the néel temperature and the entropy of the magnetic transition in the FCC phase of Fe-Mn and Fe-Mn-Co alloys *J. Alloys Compd.* **688** 594–8
[42] Adams J J, Agosta D S, Leisure R G and Ledbetter H 2006 Elastic constants of monocrystal iron from 3 to 500k *J. Appl. Phys.* **100** 113530
[43] Dever D J 1972 Temperature dependence of the elastic constants in α-iron single crystals: relationship to spin order and diffusion anomalies *J. Appl. Phys.* **43** 3293–301
[44] Wallace D C, Sidles P H and Danielson G C 1960 Specific heat of high purity iron by a pulse heating method *J. Appl. Phys.* **31** 168–76

[45] Seki I and Nagata K 2005 Lattice constant of iron and austenite including its supersaturation phase of carbon *ISIJ Int.* **45** 1789–94
[46] Stanislaw Basinski Z, Hume-Rothery W and Sutton A L 1955 The lattice expansion of iron *Proc. R. Soc.* A **229** 459–67
[47] Nix F C and MacNair D 1941 The thermal expansion of pure metals: copper, gold, aluminum, nickel and iron *Phys. Rev.* **60** 597
[48] Crangle J and Goodman G M 1971 The magnetization of pure iron and nickel *Proc. R. Soc.* A **321** 477–91
[49] Baskes M I 2000 Atomistic model of plutonium *Phys. Rev.* B **62** 15532
[50] Pauling L 1960 *The Nature of the Chemical Bond* 3rd edn (Cornell University Press)